

Section 1. PROTEIN MODELING

AMINO ACID SEQUENCE OF RECOMBINANT HUMAN PROLACTIN (PREPROTECH, CAT. 100-07, LOT 0211301)

0- MLPICPGGAA RCQVTLRDLF DRAVVLSHYI HNLSEMSE FDKRYTHGRG FITKAINSCH
TSSLATPEDK EQAQQMNQKD FLSLIVSILR SWNEPLYHLV TEVRGMQEAP EAILSKAWEI
EEQTKRLLG MELIVSQVHP ETKENEIYPV WSGLPSLQMA DEESRLSAYY NLLHCLRRDS
HKIDNYLKLL KCRIIHNNNC -200

Table S1: Prolactin SERS spectra. Characteristic Raman Bands Assignment and Amino acid Sequence

Raman Shift (cm ⁻¹)	Relative intensity	Proposed Band Assignment	References
419	W	Glutamine (409) Q Ring torsion of phenyl (447)	[28,29]
523	VVW	S-S disulfide stretching in proteins (524) v(S-S) aminoacid cysteine C	[28]
617	VS	C-C twisting (proteins) C-C twisting mode of phenylalanine (618, 621) Deformation O=C=O (phenylalanine) (606) F	[29,30]
707	W	v(C-S) trans (aminoacid methionine). P C-C stretching proline	[29]
743	W	Symmetric stretching of tryptophan (749, 759). W Deformation ring C-H, out-of-plane bending ring (748)	[29–31]
827	VVW	Out-of-plane ring breathing tyrosine (823-831). Y	[29]
920	W	Skeletal C-C, alpha-helix (932) v(C-C) skeletal backbone (933-34) C-C stretching mode of proline (911), valine (948) and protein backbone, alpha helix conformation (935)	[29,30]
950	W	Single bond stretching vibrations of proline and valine (950) v _s (CH ₃) of proteins (alpha-helix) (951). P V	[29]
1023	VVW	C-H in plane bending mode of phenylalanine (1031). F	[29]
1080	VVW	Proline (1067). P C-N stretching mode of proteins (1083)	[29]
1140	M	v(C-N) (1152) and C-C, C-N stretching (1155-56) Tyrosine (1163). Y	[29]
1170	VVW	CH bend, tyrosine and phenylalanine (1174). Y F	[29]
1240	M	Amide III, a C-N stretch from alpha-helix proteins (1258-79), random structure amide III (1250) Tryptophan (1261, 1266). W	[29-31]
1292	VVW	Amide III (1302), alpha helices (1270-1300) CH ₃ , CH ₂ twisting C-N asymmetric stretching in asymmetric aromatic amines (1308)	[29, 32]
1326	W	CH ₃ CH ₂ wagging (1335)	[29]
1353	VVW	Tryptophan (1359), hydrophobicity marker for tryptophan (1360/1340) W	[29, 32]
1405	W	v COO- (1409) Serine (1413). S	[29,30]



Figure S1: Prolactin Model Colored with Amino acid Sequence, created from Solution structure of human prolactin. PDB DOI: [https://doi.org/10.2210/pdb1RW5/pdbBMRB: 6643BMRB: 5599](https://doi.org/10.2210/pdb1RW5/pdbBMRB:6643BMRB:5599) (Berman et al., 2000; Berman et al., 2003, Teilum et al., 2005; RSCB.org)

*Alpha-helices are shown in black

H.M. Berman, J. Westbrook, Z. Feng, G. Gilliland, T.N. Bhat, H. Weissig, I.N. Shindyalov, P.E. Bourne, The Protein Data Bank (2000) *Nucleic Acids Research* 28: 235-242 <https://doi.org/10.1093/nar/28.1.235>.

H.M. Berman, K. Henrick, H. Nakamura Announcing the worldwide Protein Data Bank (2003) *Nature Structural Biology* 10:980 <https://doi.org/10.1038/nsb1203-980>.

RCSB Protein Data Bank (RCSB.org): delivery of experimentally-determined PDB structures alongside one million computed structure models of proteins from artificial intelligence/machine learning (2023) *Nucleic Acids Research* 51: D488–D508 <https://doi.org/10.1093/nar/gkac1077>

Teilum K, Hoch JC, Goffin V, Kinet S, Martial JA, Kragelund BB. Solution structure of human prolactin. *J Mol Biol.* 2005 Aug 26;351(4):810-23. doi: 10.1016/j.jmb.2005.06.042. PMID: 16045928.

Section 2. Deconvolution process of Raman spectra

The deconvolution process was performed using the Fityk program version 1.3 (Referenced in manuscript in [18]), which offers a menu of bell-shaped functions to fit the Raman bands. Some negligible effect appears in the full widths at half maximum (FWHM), which may be ignored in the overall spectral analysis. Lorentzian functions were chosen for the fit. All spectra were normalized by choosing the peak with maximum peak area and divide all other peak areas with the maximum peak area. Before the fitting was performed, careful consideration must be paid to determine as best as possible the base line of the Raman spectra. To do this, the fluorescence background was determined by fitting a polynomial curve to the measured spectrum from the points where no Raman signal is expected to be present, and this is subtracted from the original data. Normalized SERS and spectra of the samples and the background are shown in Figure S2 before this was removed.

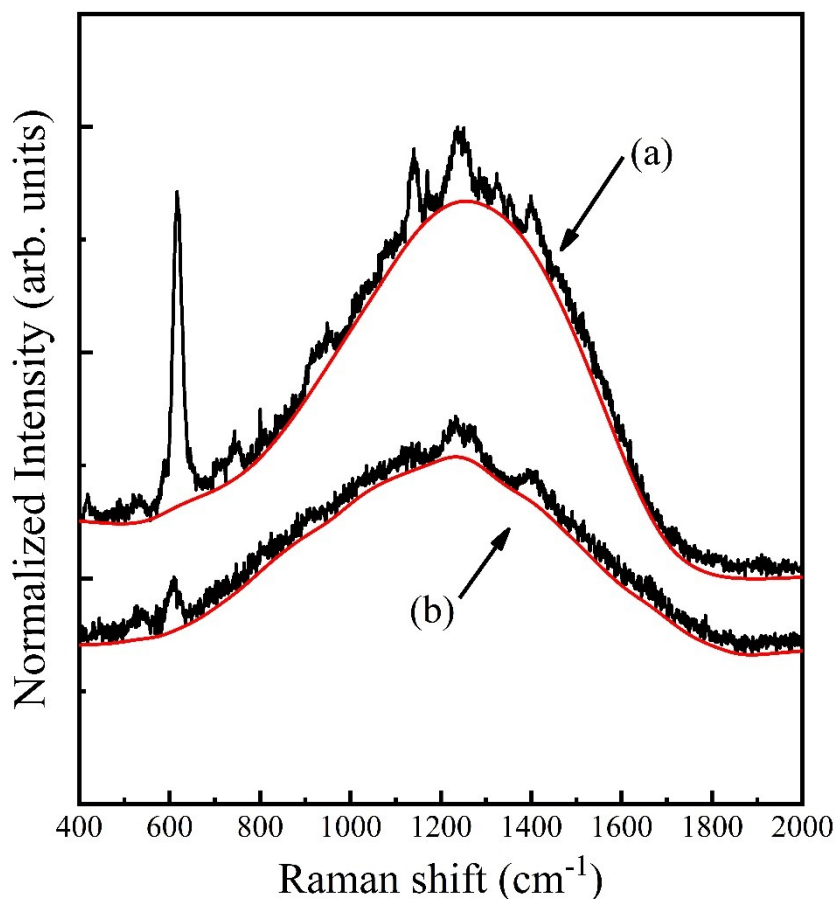


Figure S2. Normalized spectra of (a) SERS and (b) Raman spectra of Prolactin (0.0001 ng/ μ l) with fluorescence signal and the computed baseline.

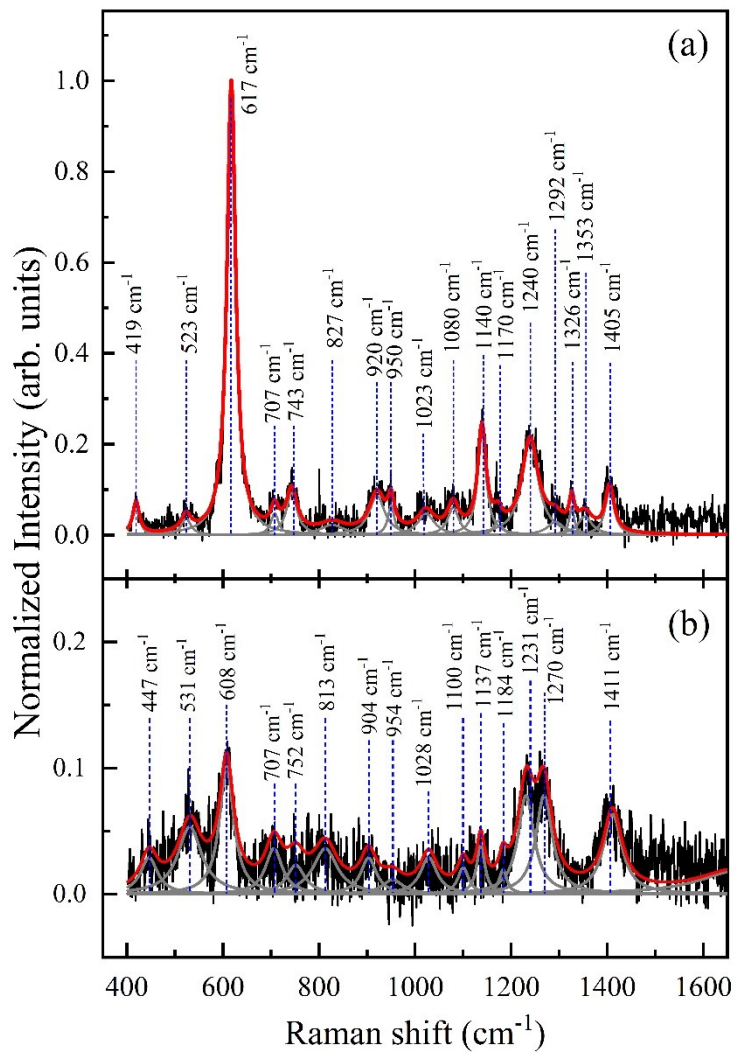


Figure S3. Normalized spectra of (a) SERS and (b) Raman spectra of Prolactin (0.0001 ng/ μ l) showing the decomposition of the spectrum using Lorentzian curves.

Table S2. Centers values in cm^{-1} and normalized intensities of the vibrational modes obtained from the theoretical fitting of the SERS spectra of prolactin at different concentrations.

PRL	0.0001 ng/ μl			0.001 ng/ μl			0.01 ng/ μl			0.1 ng/ μl			1 ng/ μl			10 ng/ μl		
	Mode number	center (cm^{-1})	Normalized Intensity (arb. Units)	center (cm^{-1})	Normalized Intensity (arb. Units)	center (cm^{-1})	Normalized Intensity (arb. Units)	center (cm^{-1})	Normalized Intensity (arb. Units)	center (cm^{-1})	Normalized Intensity (arb. Units)	center (cm^{-1})	Normalized Intensity (arb. Units)	center (cm^{-1})	Normalized Intensity (arb. Units)	center (cm^{-1})	Normalized Intensity (arb. Units)	
1	419.3	/W	7.32	423.0	/VW	1.99	407.9	/W	3.19	409.2	/W	2.47	442.5	/W	3.41	439.4	/W	3.70
2	523.4	/VW	3.82	511.1	/VVW	0.94				523.7	/VW	1.13	560.0	/W	3.22	509.9	/W	3.62
3	617.5	/VS	100.00	590.3	/VS	31.74	594.4	/VS	38.07	597.6	/VS	23.55	600.4	/VS	14.53	603.0	/VS	21.12
4	707.8	/W	5.01	701.0	/W	6.77	707.3	/W	2.82	689.8	/M	4.30	706.6	/W	3.22	702.9	/W	3.22
5	743.1	/W	9.68	723.1	/VW	1.86	744.6	/W	2.53	715.6	/W	2.83	737.0	/M	3.91	726.0	/W	3.91
6	827.6	/VW	2.35	797.0	/VVW	0.74				797.0	/M	3.61	805.6	/M	5.32	797.0	/W	4.29
7	920.5	/W	9.02	904.1	/W	6.92	890.3	/M	4.79	899.5	/W	2.66	915.7	/W	3.06	901.0	/W	5.91
8	950	/W	6.73	924.2	/VW	1.95	944.0	/VVW	0.49	921.2	/M	4.57	985.4	/W	3.41	926.9	/W	4.16
9	1023.2	/VW	4.88	1018.1	/W	5.60	1009.2	/M	4.57	1003.7	/M	4.14	1036.6	/W	2.59	1020.8	/VW	1.99
10	1079.5	/VW	6.38				1065.5	/VW	1.43							1100.8	/W	5.16
11	1139.2	/M	23.85	1121.1	/M	9.94				1145.9	/VW	1.23	1148.9	/M	3.79	1122.1	/W	5.21
12	1172.8	/VW	3.27	1196.2	/VW	2.45							1195.8	/M	3.99	1186.2	/W	4.80
13	1239.4	/M	21.53	1234.6	/M	9.54	1240.9	/VW	1.38	1247.3	/W	2.72	1245.6	/M	5.40	1217.4	/M	9.22
14	1292.6	/VW	3.06	1275.5	/VW	2.54	1274.8	/W	3.12	1297.4	/VW	1.85				1280.3	/VW	1.38
15	1326.2	/W	6.47	1325.0	/VVW	0.69	1317.0	/VW	1.12				1309.6	/VVW	1.14	1315.9	/VVW	0.93
16	1353.6	/VW	4.26	1350.7	/VW	1.38	1345.0	/VW	1.53	1342.1	/VVW	0.27	1344.5	/M	4.47	1336.5	/VW	1.50
17	1405	/W	10.71				1384.7	/W	3.53	1383.5	/VW	1.53	1381.6	/W	2.22	1392.8	/VW	1.39

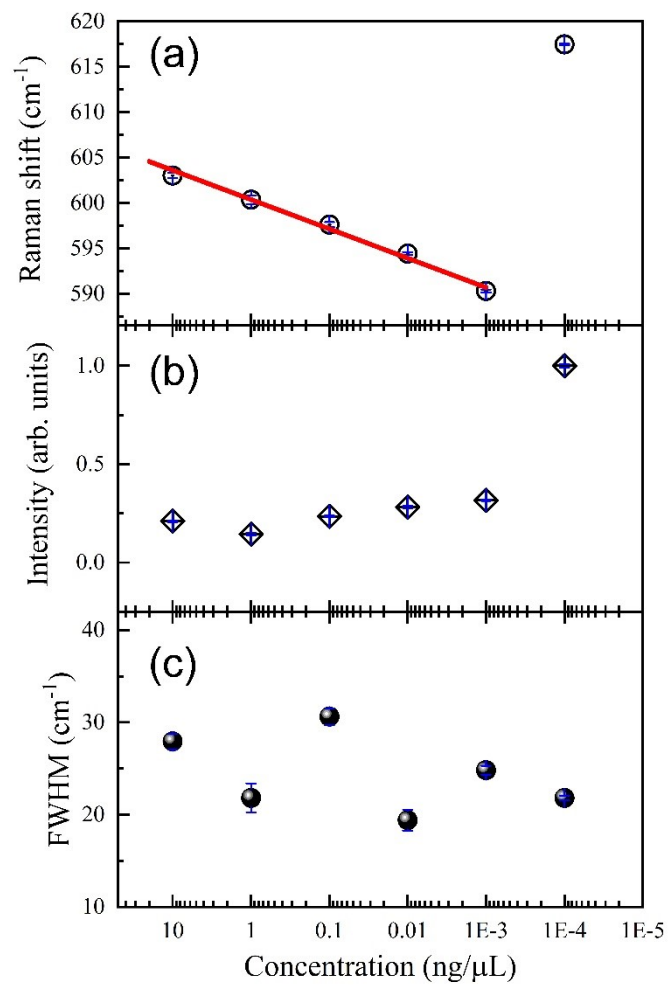


Figure S4. Raman mode corresponding to Phe signal with different Prolactin concentration for SERS experiments.

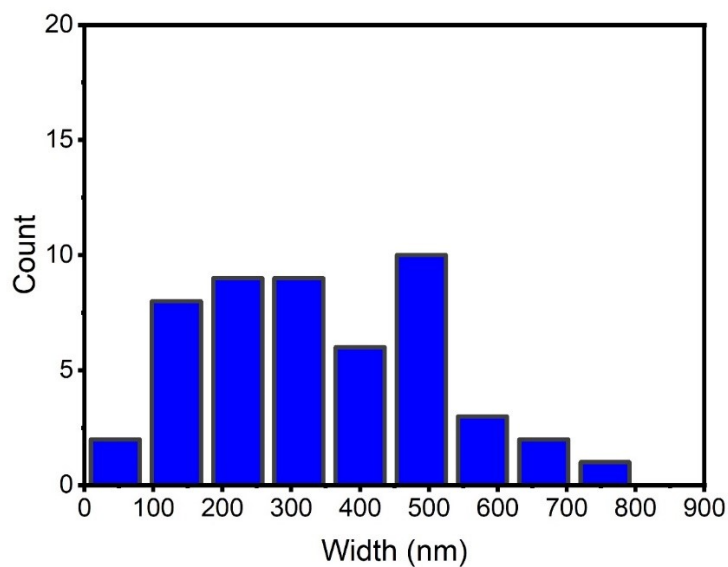
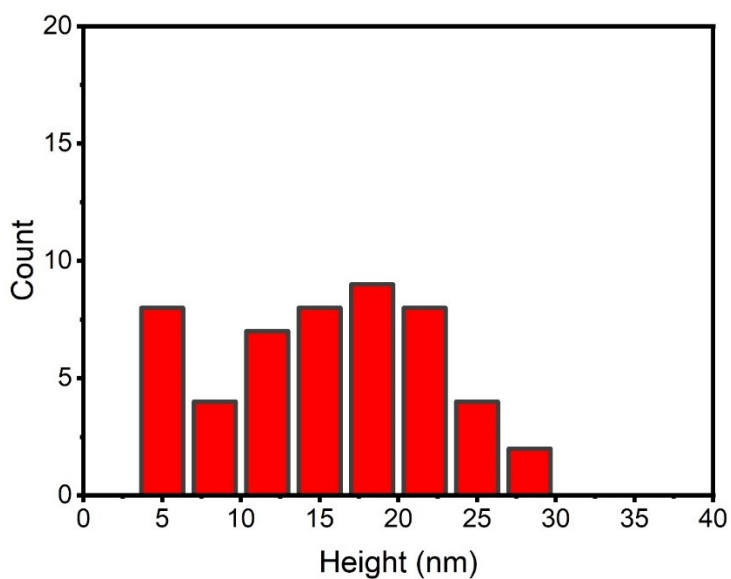


Figure S5. Histograms of nanoparticle height (red) and width (blue) measured with atomic force microscopy. As shown in Figure 2 in the text, the smaller measured nanoparticle size was about 5nm, which is expected to result from NP synthesis. However, nanoparticle aggregates were also obtained as can be observed in the size distributions of height and width.

Section 3. Search Algorithm for literature review

PubMed: Search strategy (Last update: November 8th 2023):

Prolactin + Raman; and Prolactin + Raman spectrum; Prolactin + Raman spectroscopy retrieved same 2 results; Medina-Gutiérrez et al, (2005) reported the rat prolactin spectrum, not human; and Guleken et al., (2022) who correlated serum spectra of patients with polycystic ovary syndrome and hormone levels, including prolactin. Neither of these studies reported the human prolactin Raman spectrum.

Medina-Gutiérrez C, Quintanar JL, Frausto-Reyes C, Sato-Berrú R. The application of NIR Raman spectroscopy in the assessment of serum thyroid-stimulating hormone in rats. *Spectrochim Acta A Mol Biomol Spectrosc.* 2005 Jan 1;61(1-2):87-91. doi: 10.1016/j.saa.2004.03.016. PMID: 15556425.

Guleken Z, Bulut H, Bulut B, Paja W, Orzechowska B, Parlinska-Wojtan M, Depciuch J. Identification of polycystic ovary syndrome from blood serum using hormone levels via Raman spectroscopy and multivariate analysis. *Spectrochim Acta A Mol Biomol Spectrosc.* 2022 May 15;273:121029. doi: 10.1016/j.saa.2022.121029. Epub 2022 Feb 18. PMID: 35217265.

Prolactin + SERS retrieved zero results.

PMC: ("prolactin"[MeSH Terms] OR "prolactin"[All Fields]) AND ("spectrum analysis, raman"[MeSH Terms] OR ("spectrum"[All Fields] AND "analysis"[All Fields] AND "raman"[All Fields]) OR "raman spectrum analysis"[All Fields] OR ("raman"[All Fields] AND "spectroscopy"[All Fields]) OR "raman spectroscopy"[All Fields]).

Retrieved 185 results.

After verifying titles, abstracts and figures, we corroborate that none of them reported the human prolactin Raman spectrum.

Two of the retrieved results are about Raman spectroscopy in biofluids and its correlation with prolactin serum levels:

Huang X, Hong L, Wu Y, Chen M, Kong P, Ruan J, Teng X, Wei Z. Raman Spectrum of Follicular Fluid: A Potential Biomarker for Oocyte Developmental Competence in Polycystic Ovary Syndrome. *Front Cell Dev Biol.* 2021 Nov 11;9:777224. doi: 10.3389/fcell.2021.777224. PMID: 34858993; PMCID: PMC8632455.

Hu D, Wang J, Cheng T, Li H, Zhang F, Zhao D, Xu X, Yu R, Wen P, Cheng Y, Xu J, Jin L, Yao J. Comparative analysis of serum and saliva samples using Raman spectroscopy: a high-throughput investigation in patients with polycystic ovary syndrome and periodontitis. *BMC Womens Health.* 2023 Oct 4;23(1):522. doi: 10.1186/s12905-023-02663-y. PMID: 37794378; PMCID: PMC10552415.

Section 4. Design Model of Aluminum Device used in the Raman Measurements

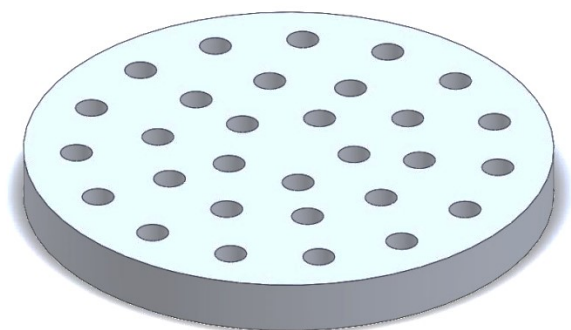


Figure S6.- *Schematic Model of Aluminium sample holder.*